The Magnetocaloric Effect of $LaFe_{11.6}Si_{1.4}$, $La_{0.8}Nd_{0.2}Fe_{11.5}Si_{1.5}$, and $Ni_{43}Mn_{46}Sn_{11}$ Compounds in the Vicinity of the First-Order Phase Transition

By *Jun-Ding Zou, Bao-Gen Shen,* Bo Gao, Jun Shen,* and *Ji-Rong Sun*

The magnetocaloric effect (MCE), found by Warburg,[1] provides a unique way for realizing refrigeration from ultralow temperatures to room temperature. With an increase of applied field, the magnetic entropy decreases and heat is emitted from the magnetic system to the environment in an isothermal process; with a decrease of applied field, the magnetic entropy increases and heat is absorbed from the lattice system to the magnetic system in an adiabatic process. Both the large, isothermal entropy change and the adiabatic temperature change characterize the prominent MCE. Over the past few years, the MCE and magnetic refrigeration materials have been investigated extensively,[2–13] and several kinds of magnetic-refrigerant prototype instruments have been implemented experimentally.[14–16] However, the origin and evaluation method of the MCE are still in dispute. Here, we will start from the thermodynamic deduction, then combine magnetic and caloric measurements to study the MCE in the vicinity of the first-order phase transition.

Usually, the MCE can be observed through magnetic or calorimetric measurements. The method of magnetic measurements based on the Maxwell relation is accepted widely, although it is still controversial. The bone of contention seems to be whether the rate of change of the magnetization with temperature, $\partial M/\partial T$, is finite. Giguère et al.[17] and Földeàki et al.[18] pointed out that as $\partial M/\partial T$ is infinite during a first-order phase transition, the Maxwell relation is not suitable for calculating the entropy change in such a case. On the contrary, Gschneidner et al.,[19] Sun et al.[20] and Wada et al.[21] claimed that $\partial M/\partial T$ is finite in real materials and the Maxwell relation is applicable. Currently, the Maxwell relation is widely used to calculate the MCE. Recent advances in MCE research of MnAs[11] and $Mn_{(1-x)}Fe_xAs$[12] have aroused one to reconsider the origin and the evaluation method of the MCE in the case of a first-order phase transition. Entropy changes, observed in MnAs (under a static pressure)[11] and $Mn_{(1-x)}Fe_xAs$ (at ambient pressure)[12] are much larger than the theoretical limitations, and are referred to as the colossal MCE. It is worth noting that sharp ''spikes'' appear in the entropy-change curves in many reports on giant or colossal MCEs, whether the measurements are under a strong or weak applied field.[2–4,6,11,12]

One possible origin for the ''spikes'' may be the coexistence of paramagnetic (PM) and ferromagnetic (FM) phases.[22] We do not think that the relationship between the MCE and a ''spike'' has been entirely established yet. Therefore, the thermodynamics relations must be carefully analyzed so as to clarify the problem thoroughly. We detail the process of deducing the Maxwell relation and its necessary conditions, and then apply it to the discussion of $LaFe_{11.6}Si_{1.4}$, $La_{0.8}Nd_{0.2}Fe_{11.5}Si_{1.5}$, and $Ni_{43}Mn_{46}Sn_{11}$ compounds.

Deducing the thermodynamics relations are important and helpful for an understanding of the origin of the ''spikes'' in the entropy-change curves. For a reversible process, the internal energy of a paramagnet is given by Equation (1):

$$dU(M, V, S) = HdM - PdV + TdS \tag{1}$$

In Equation (1), U is the internal energy, M is the magnetization, V is the volume, S is the entropy, H is the applied field, P is the pressure, and T is the temperature. After a Legendre transformation, Equation (1) takes the form described in Equation (2):

$$G = U - MH + PV - TS \tag{2}$$

In Equation (2), G is the Gibbs free enthalpy. If the second-order mixed partial derivative of G is continuous, it is easy to obtain the Maxwell relation (Equation (3)):

$$\begin{cases} \left(\frac{\partial V}{\partial H}\right)_{P,T} = -\left(\frac{\partial M}{\partial P}\right)_{H,T} \\ \left(\frac{\partial V}{\partial T}\right)_{P,H} = -\left(\frac{\partial S}{\partial P}\right)_{H,T} \\ \left(\frac{\partial M}{\partial T}\right)_{P,H} = \left(\frac{\partial S}{\partial H}\right)_{P,T} \end{cases} \tag{3}$$

If the magnetic system can be regarded as being independent, the magnetic entropy change under an applied field can be expressed as shown in Equation (4):

$$\Delta S = S(H_1, T) - S(H_0, T) = \int_{H_0}^{H_1} \left(\frac{\partial M}{\partial T}\right)_H dH \tag{4}$$

[*] Dr. J. Zou, B. Gao, J. Shen, Prof. J. Sun, Prof. B. Shen
State Key Laboratory for Magnetism
Institute of Physics
Chinese Academy of Sciences
Beijing 100190 (China)
E-mail: shenbg@g203.iphy.ac.cn

DOI: 10.1002/adma.200800955

Equation (4) is widely used to calculate the entropy change. In fact, Equation (4) can be integrated numerically, and presented in the following form (Equation (5)):

$$-\Delta S = \sum_i \frac{1}{T_{i+1} - T_i}(M_i - M_{i+1})\Delta H_i \quad (5)$$

It is well known that first-order magnetic phase transitions are often accompanied by volume deformation. It is an indication that strong couplings exist, such as the magnetoelastic coupling, so the results calculated from Equation (4) and (5) give the total entropy change of the system (see to Equation (1–3)).

According to thermodynamics, it is easy to attain the relationship between the entropy and the heat capacity as expressed below in Equation (6):

$$\Delta S(T) = \int_0^T \frac{C_H(T) - C_0(T)}{T} dT \quad (6)$$

Equation (6) is used to calculate the MCE through heat-capacity measurements. The result calculated from Equation (6) is the total entropy change in real materials, and is the same as that calculated from Equation (4) and (5).

Now, we would like to discuss the entropy change in $LaFe_{11.6}Si_{1.4}$, $La_{0.8}Nd_{0.2}Fe_{11.5}Si_{1.5}$ and $Ni_{43}Mn_{46}Sn_{11}$. For the purpose of the MCE estimation, we have measured the isothermal magnetization curves and calculated the entropy change from Equation (5). The sketch calculation is shown in Scheme 1, in which T_1, T_2 and T_3 are temperatures, and Σ_1, Σ_2 and Σ_3 are the areas bounded by the curves at T_1, T_2 and T_3. The entropy change at a temperature of $(T_1 + T_2)/2$ is given by Equation (7):

$$\Delta S\left(\frac{T_1 + T_2}{2}\right) = \frac{\Sigma_1}{T_2 - T_1} \quad (7)$$

It is clear that the magnitude of ΔS corresponds to the area, Σ.

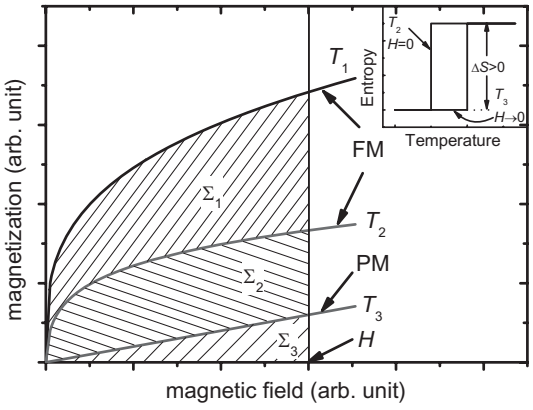

Scheme 1. Schematic diagram of the isothermal magnetizations; T_1, T_2 and T_3 are the temperatures. The shadowed areas Σ_i ($i = 1, 2, 3$) are used to calculate the entropy change by using the Maxwell relation. H is the applied field. The inset shows the entropy plotted against temperature when T_C is equal to $(T_2 + T_3)/2$.

Isothermal magnetization curves for $LaFe_{11.6}Si_{1.4}$ measured from 180 to 220 K, with the applied field increasing from 0 to 5 T, are shown in Figure 1a. Σ_i ($i = 1, 2, ..., 10$) denotes the area bounded by two adjacent M–H curves. The entropy changes calculated from the Maxwell relation are shown in Figure 1b. The peak value was 37 J K^{-1} kg^{-1} at 0–5 T. The corresponding results for $La_{0.8}Nd_{0.2}Fe_{11.5}Si_{1.5}$ are shown in Figure 1c and 1d. The peak value was 53 J K^{-1} kg^{-1} at 0–5 T. Nd doping causes the Curie temperature to decrease. The ''spikes'' are prominent. Note that no ''spikes'' are observed at all on entropy-change curves determined by means of the heat capacity method.[22,23] The coexistence of a FM and a PM phase, represented by the blue line in Figure 1c, was once considered to be responsible for the appearance of ''spikes''.[22] In fact, the physical picture behind the sharp ''spikes'' has not yet been fully obtained. According to Equation (7), the entropy change is in one-to-one correspondence with the area. The red arrows show these correspondences. It is clear that the ''spike'' originates from the Σ that is anomalously larger than any other Σ_i (see Σ_1 in Fig. 1a and Σ_2 in Fig. 1c). This behavior can be seen in most of the giant or colossal MCE materials, although it has not received much attention.

Considering Equation (7), if the applied field tends to zero, the area, Σ, should be close to zero. However, the ΔS will maintain a finite value at $T_C = (T_2 + T_3)/2$ for an ideal first-order phase transition, which conflicts with the result from Equation (7) (see the inset in Scheme 1). In fact, ΔS does not correspond to Σ well before the applied field is saturated. The Maxwell relation may not hold true in this case, due in part to the magnetic domain. Before becoming saturated, the applied field drives both magnetic moments and magnetic domains toward the applied field. For materials in the FM state, though the magnetizations are changed rapidly with increasing applied field, the magnetic entropies are not changed much because the macroscopic magnetization does not represent the magnetic order directly. As a result, Σ_1 in Figure 1a may be anomalously larger than any other Σ_i, which leads to the appearance of the ''spike'' (the same as Σ_2 in Fig. 1c). In contrast, when FM materials are under a saturated field, the applied field can drive the magnetic moments directly, and the domain effect is approximately negligible. Thus, the MCE estimated from the Maxwell relation is true in this case. It is easy to draw a conclusion that the Maxwell relation is applicable when the magnetic moments are freely manipulated by the applied field. This means that the Maxwell relation can be used in the case of a PM or FM state under a saturated field.

The entropy change determined using the heat capacity method is convincing. The heat capacity of the $LaFe_{11.6}Si_{1.4}$ compound has been plotted against temperature and is shown in Figure 2a. The entropy changes under different saturated fields determined by the heat capacity and the Maxwell relation are shown in Figure 2b. The heat capacity and entropy changes of $La_{0.8}Nd_{0.2}Fe_{11.5}Si_{1.5}$ are shown in Figure 2c and 2d, respectively. It is clear that the entropy change determined by using the heat capacity method dovetails with that from the Maxwell relation. The above-mentioned discussion can win complete support.

The discussions can be generalized to a Heusler-type NiMnSn alloy,[24–26] which is helpful to uncover the origin of the MCE in the NiMnSn alloy. Different to $LaFe_{11.6}Si_{1.4}$ and

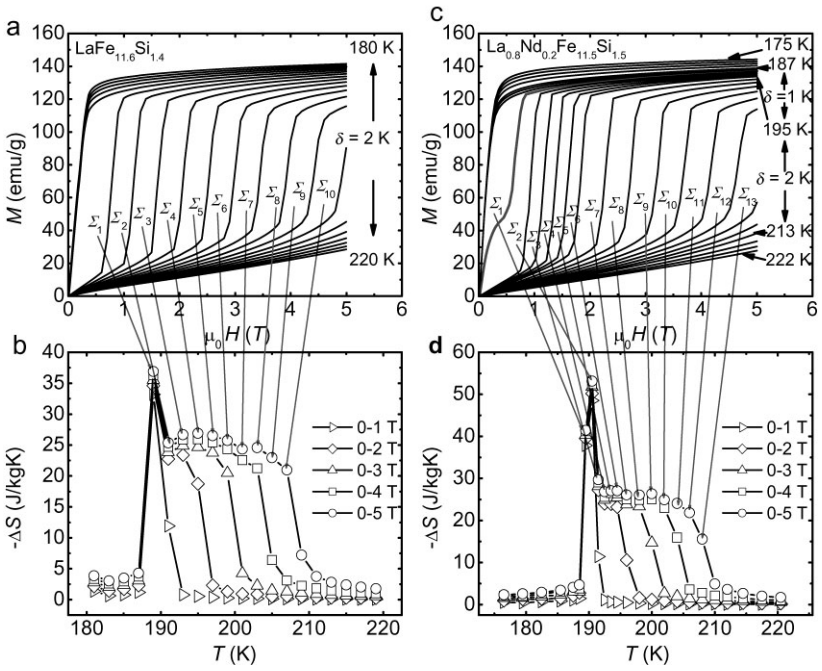

Figure 1. a) Isothermal magnetizations of $LaFe_{11.6}Si_{1.4}$ compound versus applied field, where the magnetizations were measured at increasing magnetic field. b) Temperature dependence of total entropy changes under different applied fields. c) and d) The corresponding results for $La_{0.8}Nd_{0.2}Fe_{11.5}Si_{1.5}$ compound. The red arrows indicate the correspondence between the area, Σ_i, and the entropy change; the blue line denotes FM and PM phase coexistence.

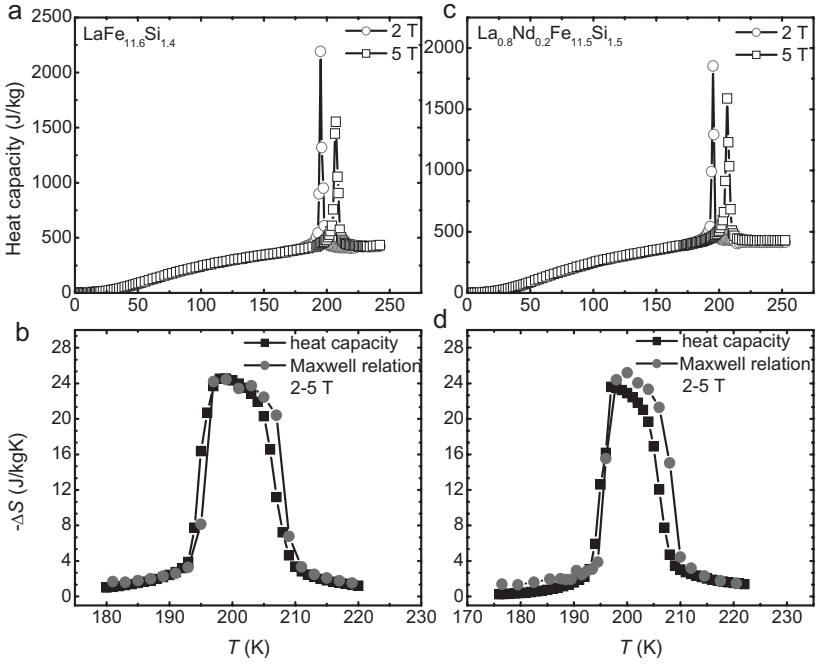

Figure 2. a) The heat capacity of $LaFe_{11.6}Si_{1.4}$ as a function of temperature and magnetic field from 2 to 242 K. b) The temperature dependence of the entropy changes of $LaFe_{11.6}Si_{1.4}$ calculated from the heat capacity (squares) and Maxwell relation (circles). c) and d) The corresponding results for $La_{0.8}Nd_{0.2}Fe_{11.5}Si_{1.5}$. The temperature interval of the heat capacity is 1 K in the vicinity of phase transition.

$La_{0.8}Nd_{0.2}Fe_{11.5}Si_{1.5}$, the giant MCE of the $Ni_{43}Mn_{46}Sn_{11}$ alloy originates from a martensitic phase transition. Previous reports[24,26] have shown that the giant inverse MCE is observed, due to modifications in the magnetic exchange interaction during the martensitic phase transition. Figure 3a shows the isothermal magnetization curves obtained between 184 and 200 K, where Σ_i ($i = 1, 2, 3, 4$) denotes the area bounded by two adjacent M–H curves. Figure 3b shows the entropy changes calculated from the Maxwell relation. The giant inverse MCE appears and the entropy-change peak reaches 78 J K^{-1} kg^{-1} for $\Delta H = 5$ T. Figure 3c shows the heat capacity of the $Ni_{43}Mn_{46}Sn_{11}$ alloy. The martensitic phase-transition temperature decreases with the increase of applied field. The entropy changes determined by the heat capacity and the Maxwell relation are shown in Figure 3d. The entropy change under a saturated applied field, determined by the heat capacity and the Maxwell relation shows a great discrepancy. The entropy change determined from the heat capacity is 2.6 J K^{-1} kg^{-1}, whereas it is 46.9 J K^{-1} kg^{-1} determined from the Maxwell relation. The reason may be that the case of the $Ni_{43}Mn_{46}Sn_{11}$ alloy does not match the requirements for employing the Maxwell relation, whether the applied field is saturated or not. It should not be neglected that the change of macroscopic magnetization does not exactly reflect the change of magnetic order in the vicinity of the martensitic phase transition. In other words, the activities of the magnetic moments are not directly manipulated by the applied field. The reasons may be the magnetic domain effect and the low-magnetization martensitic phase. If these details are ignored, misjudgment will be inevitable. Moreover, the discrepancy of the entropy change between the magnetic and caloric measurements may indicate that the magnetic state of martensitic phase is not paramagnetic.

Even now some fundamental problems in MCE research may still be unknown, though a large number of studies on the MCE and MCE materials have been carried out. $LaFe_{11.6}Si_{1.4}$, $La_{0.8}Nd_{0.2}Fe_{11.5}Si_{1.5}$ and $Ni_{43}Mn_{46}Sn_{11}$ compounds have been systematically studied to demonstrate the proper ways to evaluate the MCE and clarify the truth in MCE research. The magnetic domains and the discrepancy between the macroscopic magnetization and magnetic order are ignored, which leads to having to revaluate the results determined by magnetic measurements in the vicinity of a first-order phase transition. The anomalous enlargement in the area bounded by two adjacent M–H curves is, in part, responsible for the appearance of a "spike" on the ΔS–T curve. According to

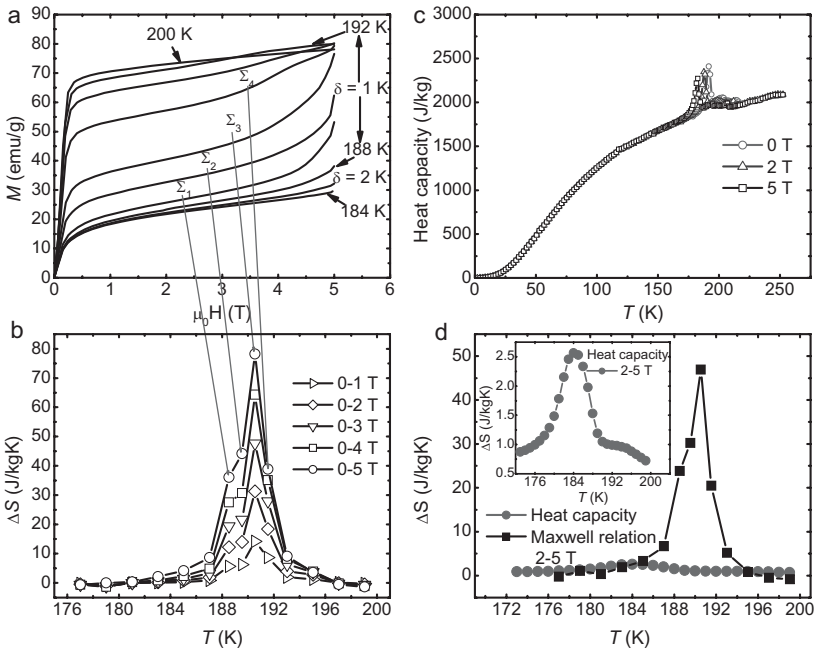

Figure 3. a) Isothermal magnetization of $Ni_{43}Mn_{46}Sn_{11}$ versus applied field, where the magnetizations are measured at an increasing magnetic field. b) The temperature dependence of the total entropy changes of $Ni_{43}Mn_{46}Sn_{11}$ under different applied fields. The red arrows indicate the correspondence between the areas, Σ_i, and the entropy change. c) The heat capacity as a function of temperature and magnetic field from 2 to 252 K. d) The temperature dependence of the entropy changes, calculated from the heat capacity (red symbols) and the Maxwell relation (black symbols). The inset shows the entropy change determined by heat capacity alone. The temperature interval of the heat capacity is 1 K in the vicinity of the phase transition.

thermodynamics, the entropy changes determined by the Maxwell relation are creditable when materials are in the PM or FM state under a saturated applied field. The case of a martensitic phase transition in $Ni_{43}Mn_{46}Sn_{11}$ alloy does not meet the necessary condition for the Maxwell relation, being responsible for the great discrepancy in the entropy change between the magnetic and heat-capacity measurements. This discussion can be easily generalized to other colossal or giant MCE materials with a first-order phase transition.

Experimental

Ingots were prepared by arc melting the pure metals under an argon atmosphere in a water-cooled copper crucible. The samples were sealed in quartz tubes at high vacuum. $LaFe_{11.6}Si_{1.4}$ and $La_{0.8}Nd_{0.2}Fe_{11.5}Si_{1.5}$ samples were annealed at 1343 K for 58 d, and then quenched in liquid nitrogen. The $Ni_{43}Mn_{46}Sn_{11}$ sample was annealed at 1173 K for 24 h, and then quenched in ice-water. The crystal structures were confirmed by X-ray powder diffraction studies at room temperature. Magnetization measurements were carried out using a superconducting quantum interference device (SQUID) magnetometer and physical properties measurement system (PPMS) from Quantum Design Inc with zero-field-cooling and fixed-point model in fields up to 5 T. Heat-capacity measurements were carried out using PPMS.

Acknowledgements

This work was supported by the National Natural Science Foundation of China, the National Basic Research Program of China, and the Basic Research Program of the Chinese Academy of Sciences. Supporting Information is available online from Wiley InterScience or from the author.

Received: April 8, 2008
Published online: November 24, 2008

[1] E. Warburg, *Ann. Phys. (Leipzig)* **1881**, *13*, 141.
[2] V. K. Pecharsky, K. A. Gschneidner, Jr., *Phys. Rev. Lett.* **1997**, *78*, 4494.
[3] V. K. Pecharsky, K. A. Gschneidner, Jr., *Appl. Phys. Lett.* **1997**, *70*, 3299.
[4] Z. B. Guo, Y. W. Du, J. S. Zhu, H. Huang, W. P. Ding, D. Feng, *Phys. Rev. Lett.* **1997**, *78*, 1142.
[5] Y. Sun, X. J. Xu, Y. H. Zhang, *J. Magn. Magn. Mater.* **2000**, *219*, 183.
[6] H. Wada, Y. Tanabe, *Appl. Phys. Lett.* **2001**, *79*, 3302.
[7] O. Tegus, E. Brück, K. H. J. Buschow, F. R. de Boer, *Nature* **2002**, *415*, 150.
[8] F. X. Hu, B. G. Shen, J. R. Sun, Z. H. Cheng, G. H. Rao, X. X. Zhang, *Appl. Phys. Lett.* **2001**, *78*, 3675.
[9] F. X. Hu, B. G. Shen, J. R. Sun, G. J. Wang, Z. H. Cheng, *Appl. Phys. Lett.* **2002**, *80*, 826.
[10] A. Fujita, S. Fujieda, Y. Hasegawa, K. Fukamichi, *Phys. Rev. B: Condens. Matter* **2003**, *67*, 104416.
[11] S. Gama, A. A. Coelho, A. de Campos, A. M. G. Carvalho, F. C. G. Gandra, P. J. von Ranke, N. A. de Oliveira, *Phys. Rev. Lett.* **2004**, *93*, 237202.
[12] A. de Campos, D. L. Rocco, A. M. G. Carvalho, L. Caron, A. A. Coelho, S. Gama, L. M. D. Silva, F. C. G. Gandra, A. O. D. Santos, L. P. Cardoso, P. J. von Ranke, N. A. de Oliveira, *Nat. Mater.* **2006**, *5*, 802.
[13] J. D. Zou, B. G. Shen, J. R. Sun, *J. Phys.: Condens. Matter* **2007**, *19*, 196220.
[14] G. V. Brown, *J. Appl. Phys.* **1976**, *47*, 3673.
[15] C. Zimm, A. Jastrab, A. Sternberg, V. Pecharsky, K. Gschneidner, Jr, M. Osborne, I. Anderson, *Adv. Cryog. Eng.* **1998**, *43*, 1759.
[16] C. Zimm, A. Boeder, J. Chell, A. Sternberg, A. Fujita, S. Fujieda, K. Fukamichi, *Int. J. Refrigeration* **2006**, *29*, 1302.
[17] A. Giguère, M. Foldeaki, B. Ravi Gopal, R. Chahine, T. K. Bose, A. Frydman, J. A. Barclay, *Phys. Rev. Lett.* **1999**, *83*, 2262.
[18] M. Földeàki, R. Chahine, T. K. Bose, J. A. Barclay, *Phys. Rev. Lett.* **2000**, *85*, 4192.
[19] K. A. Gschneidner, Jr, V. K. Pecharsky, E. Brück, H. G. M. Duijn, E. M. Levin, *Phys. Rev. Lett.* **2000**, *85*, 4190.
[20] J. R. Sun, F. X. Hu, B. G. Shen, *Phys. Rev. Lett.* **2000**, *85*, 4191.
[21] H. Wada, Y. Tanabe, M. Shiga, H. Sugawara, H. Sato, *J. Alloys Compd.* **2001**, *316*, 245.
[22] G. J. Liu, J. R. Sun, J. Shen, B. Gao, H. W. Zhang, F. X. Hu, B. G. Shen, *Appl. Phys. Lett.* **2007**, *90*, 032507.
[23] A. Giguere, M. Foldeaki, W. Schnelle, E. Gmelin, *J. Phys.: Condens. Matter* **1999**, *11*, 6969.
[24] T. Krenke, E. Duman, M. Acet, E. F. Wassermann, X. Moya, L. Mañosa, A. Planes, *Nat. Mater.* **2005**, *4*, 450.
[25] K. Koyama, H. Okada, K. Watanabe, T. Kanomata, R. Kainuma, W. Ito, K. Oikawa, K. Ishida, *Appl. Phys. Lett.* **2006**, *89*, 182510.
[26] Z. D. Han, D. H. Wang, C. L. Zhang, H. C. Xuan, B. X. Gu, Y. W. Du, *Appl. Phys. Lett.* **2007**, *90*, 042507.